Cromer Shoal Chalk Beds MCZ Natural Disturbance Study

Adaptive Risk Management: MBES volumetric comparison and predictive classification study

Author(s): Hawes, Jon

Date: March 2026

Centre for Environment, Fisheries & Aquaculture Science

Cefas

Cefas Document Control

Submitted to:	Samantha Hormbrey
Date submitted:	25/03/2026
Project Manager:	Tracy Maxwell
Report compiled by:	Jon Hawes
Quality control by:	Hayden Close
Executive sign-off (approval for submission) by:	Simeon Archer-Rand
Version:	Final
Recommended citation for this report:	Hawes, J. (2026) Cromer Shoal Chalk Beds MCZ Natural Disturbance Study- Adaptive Risk Management: MBES volumetric comparison and predictive classification.

Version control history

Version	Author	Date	Comment
0.01	Jon Hawes	23/03/2026	First Draft
0.02	Hayden Close	24/03/2026	Tech QC
1.0	Simeon Archer-Rand	24/03/2026	Exec Sign Off
Final	Jon Hawes	14/04/2026	Final
Final	Jon Hawes	20/04/2026	Maps updated

Author contributions

[Please insert a description of author contributions and responsibilities below this text. The required format is described in the embedded file. After listing author contributions and responsibilities, please delete the embedded file and this text in the square brackets]

Contribution category	Author
Design and funding acquisition	Jon Hawes
Methods development	Jon Hawes
Data and evidence collection	Jon Hawes
Data analysis and visualisation	Jon Hawes
Writing	Jon Hawes

Contents

Figures

Tables

1. Introduction

1.1. Site overview

The Cromer Shoal Chalk Beds Marine Conservation Zone (CSCB MCZ, Figure 1) along the north Norfolk coast is one of the most ecologically significant Marine Protected Areas for chalk habitats in the UK and Europe. It was designated in 2016 as part of Tranche 2 of the MCZ designation process under the Marine and Coastal Access Act (MCAA) 2009.

The MCZ was designated for nine chalk, rocky, sedimentary habitats, and a geological feature. The conservation objectives for those features were set as 'maintain in favourable condition' based on best available evidence at the time.

The chalk beds are also home to a nationally significant crab and lobster industry which is crucial to the heritage, character and economy of the north Norfolk coast.

In 2018 NE received new evidence that the local crab and lobster fishery was impacting the physical structure of the chalk bed through potting activity, and during 2019 NEs Norfolk Coast and Marine Team in partnership with others collected evidence on the impact of the potting fishery on the chalk bed. The chalk bed was found to have numerous occurrences of impact and as a result NE are continuing to work with partners over the coming years to gain a greater understanding of this impact in the context of the crustacean fishery and any potential mitigation strategies that can be employed.

Figure 1 shows the extent of the experimental areas investigated by the Natural Disturbance Study (NDS) study.

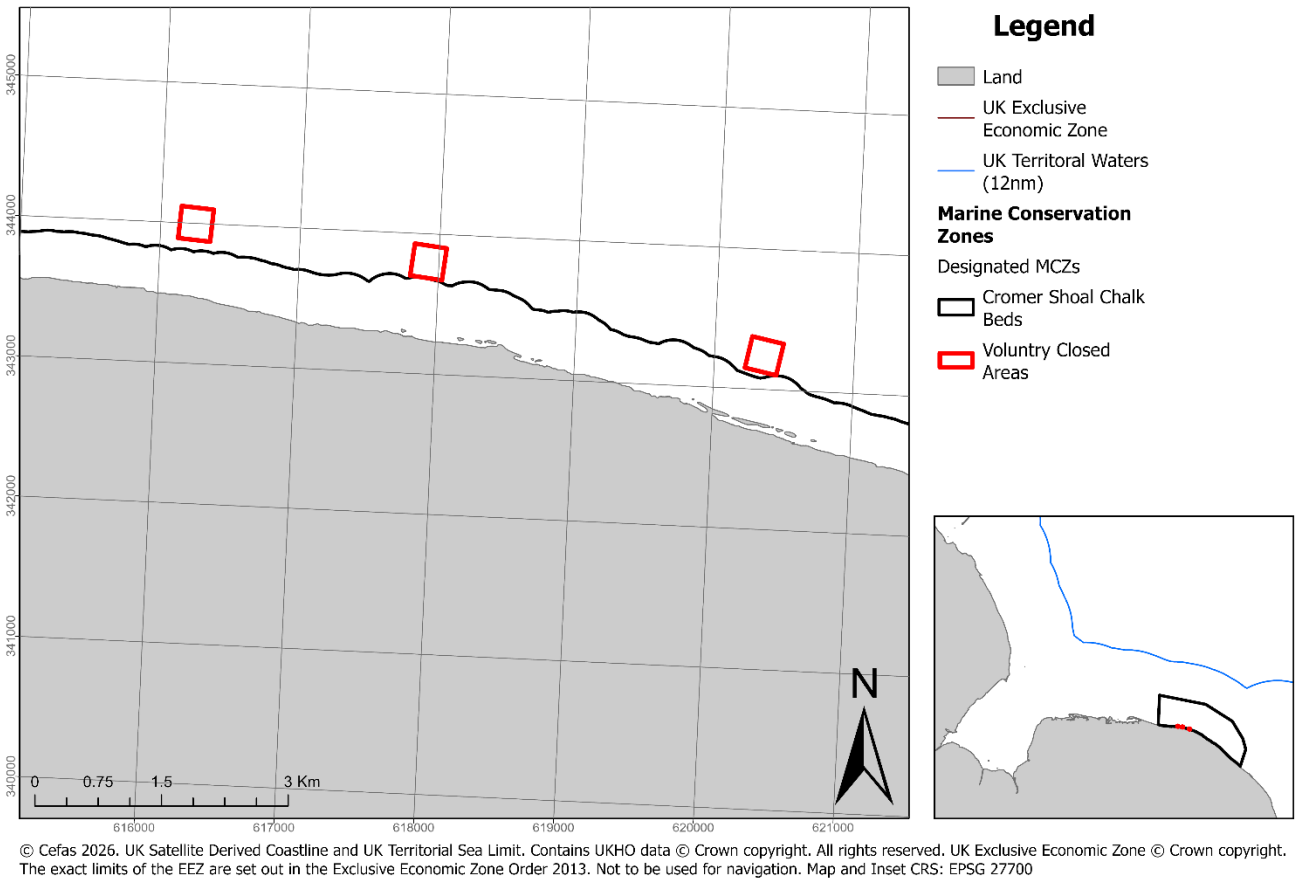

Figure 1 Map showing the extents of the experimental areas

1.2. Aims and Objectives

1.2.1. Overarching Natural Disturbance Study (Adaptive Risk Management) Project Aims

There is an identified knowledge gap pertaining to the possible physical, abrasive impacts of creel fishing methods (crab and lobster "parlour pots") on the outcropping (elevated) chalk reef designated feature of the MCZ. To address this and inform Adaptive Risk Management of the site, Eastern Inshore Fisheries Conservation Authority (EIFCA) have developed an investigative research study with the primary aim of answering the following research question:

Is there an observed difference in chalk degradation in areas of rugged chalk exposed to potting activity when compared to areas closed to potting activities?

The wider study approach is an Impact-Control methodology, testing two nested area-based treatments (Open and Closed) within three sites; East, Middle and West. Each site has a 150m^2 area delineated as open to fishing, and a 150m^2 area under a voluntary closed areas impact measure. Resulting in six 150m^2 sites undergoing monitoring.

1.2.2. Objectives of this report

In order to assess aim of the broader study (to compare changes in seabed structure and habitat rugosity between treatments and over time), this report and data processing contract has been issued. This report therefore has the following objectives:

- Process multibeam backscatter data using the Fledermaus Geocoder Toolbox (FMGT).
- Perform volumetric and structural complexity analysis (rugosity, relief, slope, etc.) by creating topographic derivative layers using ArcGIS Pro, QGIS and WhiteBox programmes
- Calculate bathymetric surface difference maps (i.e. volumetric difference layers) between each of the three datasets, representing different time points.
- Using Object Based Image Analysis (OBIA) in Trimble eCognition 10 and a custom Python 3 environment, we will create predictive habitat classification maps from a single bathymetric dataset (likely the dataset with the temporally closest / highest quality ground truth imagery).
- Final report to contain methodologies, analysis and short discussion.
- Deliver GIS shapefiles, metadata (Marine Environmental Data and Information Network (MEDIN) compliant), and a final report (max 5000 words).

2. Methodology

2.1. Dataset selection

Upon receipt of the data from EIFCA, the processed, gridded Multibeam Echosounder (MBES) outputs (.asc files at 0.25m and 0.10m resolutions) were loaded into ArcGIS Pro v 2.9.5, noting that most (but not all) datasets had a Coordinate Reference System (CRS) of "British National Grid" (EPSY WKID 27700).

Initial visual review of these datasets provided for a high level cut off of data suitability for comparative volumetric analyses and predictive classification. Table 1 provides a summary of the acoustic surveys and their indicative quality, detailing issues and utility in the present study.

Table 1 Summary of the acoustic surveys and corresponding data products acquired from the as part of this study

Dataset name	Survey Timepoint	Quality Assessment 10cm	Quality Assessment 25cm	Utilised in this report?
2024_05_17_MB	Spring 2024	Sounding density insufficient	Large gap in Middle_West	Y (East and West Baseline / "T0")
2024_10_31_MB	Autumn 2024	Sounding density insufficient	Small gap in Middle_West	Y (Middle Baseline / "T0")
2025_03_04_MB	Spring 2025	Sounding density insufficient, extensive "block" and line artefacts	Extensive "block" and line artefacts	N
2025_09_29_MB	Autumn 2025	Sounding density insufficient	Good	Y (East, Middle and West "T1")
2025_10_01_MB	Autumn 2025	Sounding density insufficient	Good	

The initial quality review focussed on gridded sounding density and coverage. The sounding density of the 0.1m gridded dataset was considered unsuitable for Triangulated Irregular Network (TIN) production and masking, both critical elements in the analytical and predictive mapping workflows. As such, it was decided to undertake the bathymetric elements of this work using the 0.25m gridded datasets.

In order to meet the objective, it was determined that the volumetric comparisons should be undertaken between two points, a baseline (also known as Timepoint 0 / "T0") and an endpoint ("T1") with as greater temporal gap as possible.

Upon review, it was noted the quality of the bathymetric dataset acquired in Spring 2025 was too poor to have confidence in its use as a T1.

As such, it was decided to use the Spring 2024 dataset as T0, and the Autumn 2025 dataset as T1. However, the size of the data gap in the Middle_west area as acquired in Spring 2024 was too large to use without reducing comparability significantly. Therefore, the volumetric comparison for the middle sites has been undertaken using the Autmn 2024 dataset as T0.

2.2. Backscatter Processing

The raw bathymetric data (Qinsy ".db" files) were loaded into

Quality Positioning Services FMGT 7.11.1, alongside paired ".qpd" files (a processed file output creased by Hydrographic contractors). These matched pairs were then used to automatically assign the CRS for the FMGT project. The raw data were loaded as "time Series" soundings, each line was reviewed to ensure consistency in settings and overlap. Angular Range Analysis (ARA) was then undertaken and a full mosaic (West, Middle and East sites for each survey time point) was then processed manually at a pixel size of 0.04m.

2.3. Bathymetric Processing

Caris Hydrographic Information Processing System (HIPS) 12.0 software was used to initially view the raw bathymetric datasets, confirm geodesy and visualise the positioning of relatable features. No further processing was required after this review, meaning that all subsequent bathymetric processing and analyses were undertaken using the ASCII grids provided by EIFCA.

2.3.1. Masking

In order to ensure accuracy and functionality of subsequent analyses (i.e. volumetric comparisons and predictive classification), it was necessary to undertake a two-way masking of the gridded bathymetric datasets. This ensured the exact same extents (including holes) of the T0 and T1 MBES grids and then further masking these grids by their processed backscatter (which may differ in their extent from the MBES due to processing requirements).

2.3.2. TIN Production

The ASCII bathymetric grids were then used to create TIN surfaces, with a maximum node number of 5,000,000 and a Z tolerance of 1cm.

2.4. Bathymetric difference

Bathymetric difference (elevation) was initially planned to be assessed on a volumetric basis, however initial results (discussed in Section 3 below) require further investigation using bathymetric profile-based analysis.

2.4.1. Surface Differences (Volumetric)

The Surface Difference tool works by comparing two input TIN surfaces in a fully geometric way, breaking them down into their component triangles and evaluating how those triangles relate to one another in three-dimensional space. When intersections occur, the tool subdivides those triangles into smaller pieces so that each portion can be cleanly categorised. Once every piece has been assigned to its correct class, the tool groups neighbouring pieces with the same classification into larger polygons. These polygons become the basis for calculating the volumetric differences between the surfaces, and the resulting areas and volumes are written to the output polygon feature class.

While doing this, the tool constructs a "difference surface" using constrained Delaunay triangulation. This surface is essentially a third TIN that represents the vertical separation between the two input surfaces. Its z-values indicate the magnitude and direction of the difference: values of zero mark locations where the two surfaces coincide; positive z-values indicate that the first surface stands above the reference; and negative values indicate it lies below. This difference surface is the foundation for generating additional outputs. If the user requests a raster rather than a polygon layer, the triangulated surface

is simply interpolated linearly into a continuous raster dataset. If the user has chosen to output a TIN, the tool writes the difference surface directly as a TIN to the designated workspace. In cases where the triangulation becomes too large for a single TIN to store, the tool automatically splits it into multiple TINs to ensure the output remains valid.

2.4.2. Bathymetric Profiles

High resolution bathymetric elevation profiles were extracted from the T0 and T1 bathymetry grids using the Stack Profile tool in the ArcGIS Pro "3D Analyst" toolkit. These profiles were based upon the as-driven ROV transects from the 2024 ground truthing survey, so that they could, in future, be related directly to the impacts to the chalk reef features observed from those imagery analyses.

A custom Python 3 script was then written and executed in Jupyter Notebook to undertake the following:

- Sets of 2024 and 2025 observations were extracted by filtering on SRC_NAME.
- Distance vectors for each bathymetric grid were inspected for monotonicity, then sorted and cleaned.
- A common overlapping distance axis was constructed using the median sampling interval of the two bathymetric grid series.
- Elevations were interpolated onto the shared axis using linear interpolation.
- Each interpolated elevation series was smoothed using a Savitzky–Golay polynomial filter (Savitzky & Golay, 1964) to reduce local noise while preserving peaks and troughs.

Alignment of bathymetric grid Profiles using Cross-Correlation

Temporal bathymetric grids frequently exhibit small horizontal offsets due to navigation corrections, slight differences in survey geometry, or shoreline migration. Direct elevation comparison without compensating for these shifts can lead to spurious peaks, mismatched profile segments, and misleading change detection.

Profiles were aligned using normalized one-dimensional cross-correlation, a standard signal-processing method for detecting the relative displacement between two discretised signals (Lewis, 1995; Bracewell, 1999).

Cross-correlation measures similarity as one signal is shifted over another; the lag yielding the maximum correlation is interpreted as the best alignment.

For each transect:

- Both profiles were de-meaned to remove absolute elevation bias.
- Missing values were filled using linear interpolation.
- Cross-correlation was computed over a constrained lag window (±5m) to avoid unrealistic shifts.
- The lag with the maximum correlation was converted to a horizontal shift (in metres) using the sampling interval.
- The 2025 profile was translated accordingly.

Peak and Trough Detection

To characterise key morphological features local maxima and minima were extracted from the smoothed bathymetric grid series.

Peaks were identified using the find_peaks() function in the *SciPy* package, employing a prominence threshold proportional to the standard deviation of the smoothed series. Troughs were detected by applying the same method to the negated profile. For each bathymetric grid, the topmost prominent peaks and troughs were retained (typically N = 10). Local extrema provide reproducible morphological "landmarks" for between-bathymetric grid matching and serve as inputs to the Hungarian assignment step described below.

Feature Matching using the Hungarian Assignment Algorithm

After profiles are horizontally aligned, peaks and troughs from the two bathymetric grids must be paired to ensure changes in elevation are assessed at homologous morphological locations (e.g., the same crest or trough minimum).

We used the Hungarian algorithm (also known as the Kuhn–Munkres algorithm; Kuhn, 1955; Munkres, 1957), a globally optimal solution to the assignment problem.

A cost matrix was constructed based on the absolute horizontal distance between each 2024 feature and each shifted 2025 feature. The Hungarian algorithm finds the set of pairings that minimises total horizontal distance. Matches exceeding a user-defined elevation tolerance (3m) were discarded as physiographically implausible. This method ensures optimal and unbiased feature pairing, avoiding local minima and arbitrary assignment decisions.

Calculation of Elevation and Morphological Change Metrics

For each matched feature-pair the following were calculated

- Vertical change (Δz): difference in elevation between years
- Residual horizontal offset: indicator of remaining misalignment
- Curvature similarity: second derivative difference, capturing shape consistency
- Confidence metrics: derived from alignment precision, vertical difference similarity, and curvature agreement to quantify uncertainty in each match

These metrics provide robust localised indicators of geomorphic change, reducing noise introduced by non-homologous comparisons.

2.4.3. Statistical Testing

Because each transect produces multiple matched features, the data are hierarchical and unbalanced:

- Multiple observations (matched pairs) per transect
- Unequal numbers of matches across transects
- Transects differ in baseline morphology and variance
- Additional grouping (Control vs Impact) from the new Before–After–Control–Impact (BACI) column

Traditional (Analysis of Variance) (ANOVA) or paired t-tests are therefore inappropriate because they cannot accommodate random effects or unbalanced grouped data structures.

Linear Mixed-Effects Models (LMMs) provide a flexible and statistically rigorous framework for such datasets. An LMM was designed to test the following null hypothesis

H_o = There is no overall vertical change between bathymetric grids across the study area.

The LMM model structure is as follows:

$$\Delta z_{ij} = \beta_0 + u_j + \epsilon_{ij}$$

Where:

- Δz_{ij}: elevation difference at matched feature i in transect j
- β_0: mean elevation change across all transects
- u_j: random intercept for each transect (accounts for baseline morphology differences)
- ε_{ij}: residual error

2.5. Structural Complexity – Geomorphological habitat classification

2.5.1. Object-Based Image Analysis (OBIA)

OBIA is a two-step process consisting of segmentation and classification. The aim of segmentation is to divide an image into meaningful objects based on their spectral and spatial characteristics (Blaschke, 2010). It has also been increasingly used in seabed mapping, either for interpreting satellite imagery in shallow environments (Phinn et al., 2012); (Roelfsema et al., 2013)), or for interpreting bathymetry and other remotely sensed data (Lucieer and Lamarche, 2011); (Stephens and Diesing, 2015). In comparison to working at the pixel level, OBIA allows further characterisation based on layer values (such as mean or standard deviation), geometry and neighbour relationships. OBIA also reduces computational intensity by reducing millions of pixels into a smaller number of more meaningful objects. When using bathymetric variables, seabed mapping is more analogous to super-pixels which represent areas of homogenous values as opposed to meaningful topographic objects visible in spectral data.

Raw and derived environmental data layers used here included the finalised, masked MBES rasters, alongside similarly masked backscatter data layers.

Derivatives were calculated for each mapping level using the Whitebox Tools Open Core v2.4.0 toolset (Lindsay, 2014) and ESRI ArcGIS Pro 2.9.5. Although a number of derivatives were considered, the final suite of layers and scales used (Table 2) in either the segmentation or classification were determined based on an iterative approach based on visually assessing the mapped products using different variables.

A multi-resolution segmentation algorithm was applied to each level (raw data and derivatives) using eCognition v10. The segmentation is a bottom-up approach with image-objects iteratively merged until the homogeneity criterion is reached (termed the scale parameter) incorporating limitations based on object shape (compactness and shape parameters). The optimal parameters

and weightings were determined through an iterative process by visually assessing different segmentations to find the settings which most closely reflected real world objects.

The segmentation was bathymetrically and geomorphologically driven, with a weight of 1 applied to the bathymetry layer and 1 applied to the "RI" and slope derivative layers. Through a process of trial and error, in order to optimise object boundaries, a segmentation routing using a scale parameter (SP) of 1 with compactness (C) value of 0.9 and a shape (S) value of 0.1 was decided upon and used.

Table 2 Bathymetric derivative layers used in the segmentation and classification of the Spring 2024 and Autumn 2025 MBES data from all six experimental areas

Derivative	Description
Relative topographic position (RTP) (5-10; 40-50)	Relative topographic position (RTP) is an index of local topographic position (i.e. how elevated or low-lying a site is relative to its surroundings) and is a modification of percent elevation range (PER; PercentElevRange) and accounts for the elevation distribution. Rather than positioning the central cell's elevation solely between the filter extrema, RTP is a piece-wise function that positions the central elevation relative to the minimum (zmin), mean (μ), and maximum values (zmax), within a local neighbourhood of a user-specified size. (Newman et al., 2018)
Profile Curvature	The vertical curvature, or the rate of change in slope along a flow line, from a digital elevation model (bathymetric grid). It is the curvature of a normal section having a common tangent line with a slope line at a given point on the surface (Florinsky, 2017). The result can be either a positive or a negative value. Positive values of the index are indicative of flow acceleration while negative profile curvature values indicate flow deceleration. Profile curvature is measured in units of m-1. (Whitebox Geospatial Ltd)
Slope	The incline, or steepness, of a bathymetric surface. Measured in degrees from the horizontal. The slope for a cell in a raster is the steepest slope of a plain defined by the cell and its eight surrounding neighbours.
Plan Curvature	Plan curvature represents the curvature of the land surface in the horizontal (planimetric) direction and describes the rate of change of aspect along a contour line. Negative plan curvature values indicate divergent flow typical of ridgelines, whereas positive values indicate convergent flow common in

	valley bottoms, making it a valuable indicator of hydrological pathways and surface shaping processes.
Total Curvature	Total curvature describes the overall curvature of the surface itself rather than the curvature of intersecting lines, integrating both convexity and concavity across multiple directions. It reflects the second derivative of the Digital Elevation Model, providing a generalised measure of terrain shape that can be positive, negative, or zero depending on whether the surface locally bulges upward, downward, or displays balanced curvatures, such as at a saddle point.
Ruggedness Index (RI)	The Ruggedness Index quantifies terrain heterogeneity by calculating the mean absolute difference in elevation between a central cell and its surrounding neighbourhood, following the method of Riley et al. (1999).
Multi-scale roughness (MSR (1-2))	Multi-scale roughness (1-2 pixel window) measures variations in terrain texture by calculating surface roughness across a range of spatial neighbourhood sizes, enabling the characterisation of terrain features at different scales.

2.5.2. Predictive (classification) model generation

Predictive classification was undertaken by geomorphological description of the chalk reef features, using manually reclassified images (video frames) from the 2024 Remotely Operated Vehicle (ROV) survey (18 transects Where original image analysis by EIFCA recorded geomorphological classifications of "Rugged Chalk" and "Not Rugged Chalk", it was considered that the data set could yield a tighter and more geomorphologically apt classification. As such, images were classified after the Dove *et al.* (2020) Two Part Seabed Geomorphology Classification.

The resulting classes were:

- Gravel/ Rubble Flat (Class "0")
- Groove (Class "1")
- Mound (Class "2")
- Spur (Class "3")

Where ground truth samples (17 video tow segments from the 2024 survey) were located entirely within an object, those objects were classified based on that sample's assigned biotope. If no ground truth sample was found within that object, the object was classed as 'Unclassified'.

The segmentations were exported from eCognition v10 as shapefiles, with the attribute tables including the mean value, per object, of each of the data layers

included and a ‘class’ attribute. This resulted in a total of 401 classified segments (the training dataset), out of a total of ~29,282 objects for the Spring 2024 segmentation, and ~32,318 objects for the Autumn 2025 segmentation.

Predictive modelling was undertaken for each year separately, using a model trained on the 2024 dataset – ensuring consistency in model prediction. Training and classification was undertaken using the Python 3 machine learning library PyCaret 2.2.2, performed in Jupyter Notebook 6.1.4. The *pycaret.classification* module *setup()* function was used to first separate the data into training and testing datasets (70 / 30 %) using random sampling with proportional allocation based on class type (Olofsson, P., Foody, G.M., Herold, M., Stehman, S. V., Woodcock, C.E., Wulder, 2014). The *setup*() function allows for mixed numerical and categorical predictor classes to be incorporated into the same model testing environment and allows for unbalanced training class data (which is often the case in seabed habitat mapping with limitations on ground truth sample acquisition). Cross-validation was set to 10 folds using the ‘stratifiedKfold’ strategy. The *compare_models*() function was then used to run an iterative model creation and performance assessment process across all valid classification models within the PyCaret library. This allows for quick identification of the most applicable and accurate model type (using a variety of cross-validated performance metrics such as: producers accuracy (quality of the classification), users accuracy (probability that the prediction represents reality), Area Under the Curve (AUC), recall, precision, and Kappa) allowing the user to then create the most accurate model.

Following setup of the model building and testing algorithm (using the PyCaret *setup()* function), the *best*() function was used to train (using the specified hyperparameters) and compare a suite of all suitable classification models held within the PyCaret library. The cross-validation accuracy (10-fold) of these models was compared to determine which model was most suited to the task.

3. Results

3.1. Backscatter Datasets

The backscatter data outputs (floating point geotiff mosaics at 0.04m resolution) were of excellent quality, indicating a consistency in frequency and beam angle being adhered to during acquisition. The ranges remained broadly

consistent between surveys (T0 and T1). The resulting mosaics are presented in
Figure 2 and Figure 3.

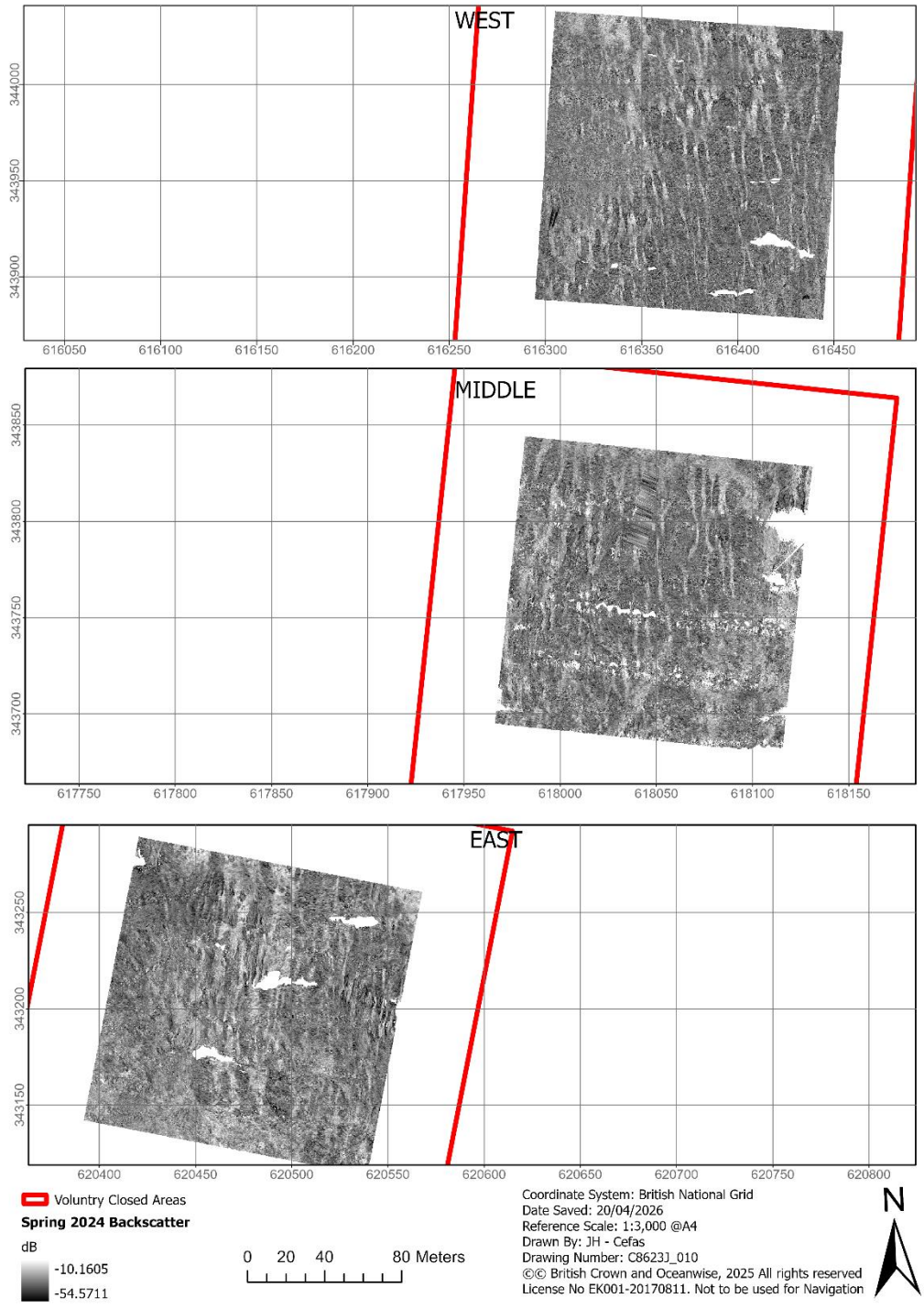

Figure 2. Map showing the masked "Spring 2024" backscatter datasets from the three experimental areas.

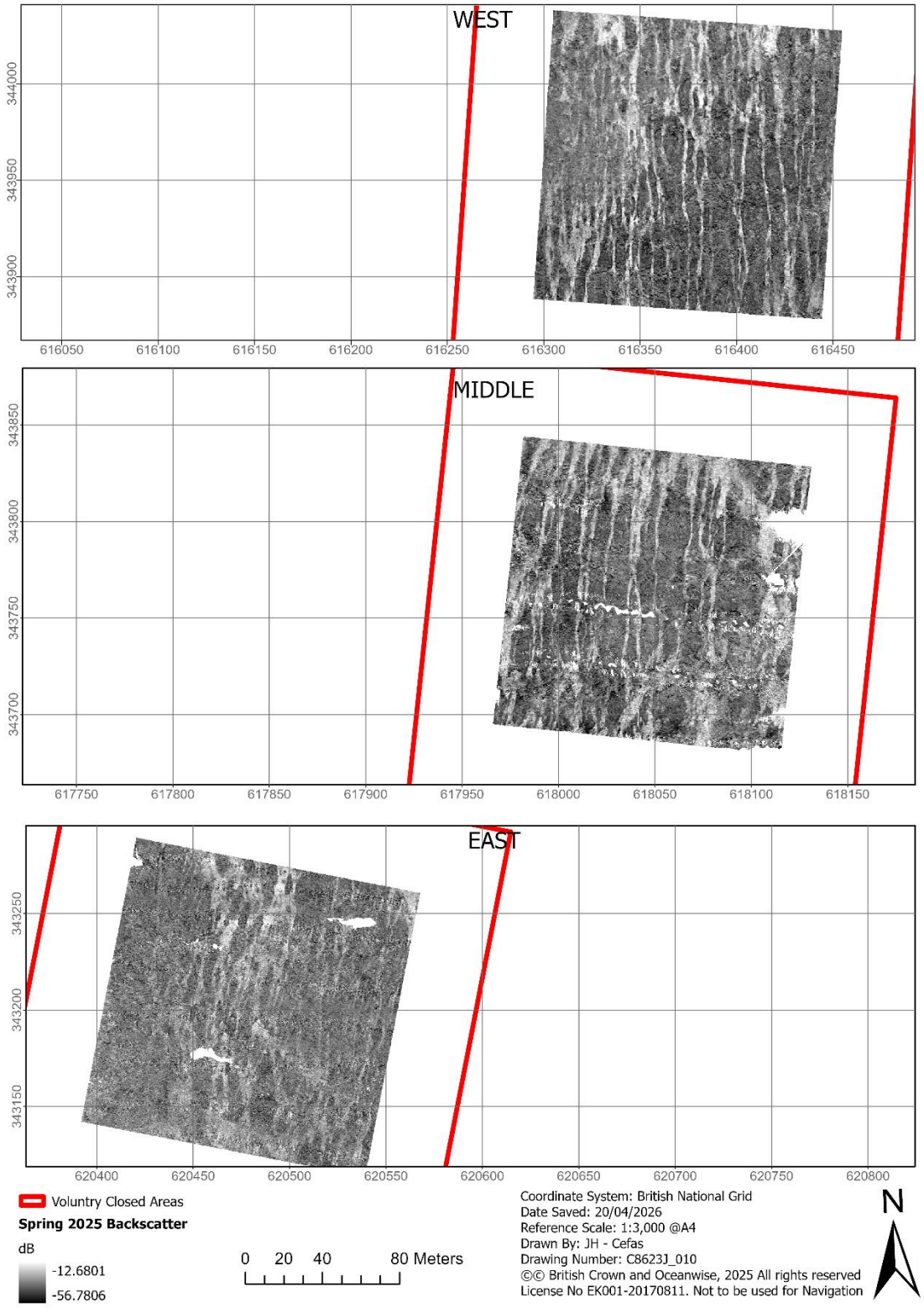

Figure 3. Map showing the masked "Autumn 2025" backscatter datasets from the three experimental areas.

3.2. Bathymetric Comparison

The masked MBES grids (0.25m resolution) which were used to create the habitat mapping derivatives and in the predictive classification, as well as in creating the final TIN datasets for surface difference calculation, have been provided as floating point geotiff mosaics. These are presented in Figure 4, Figure 5 and Figure 6.

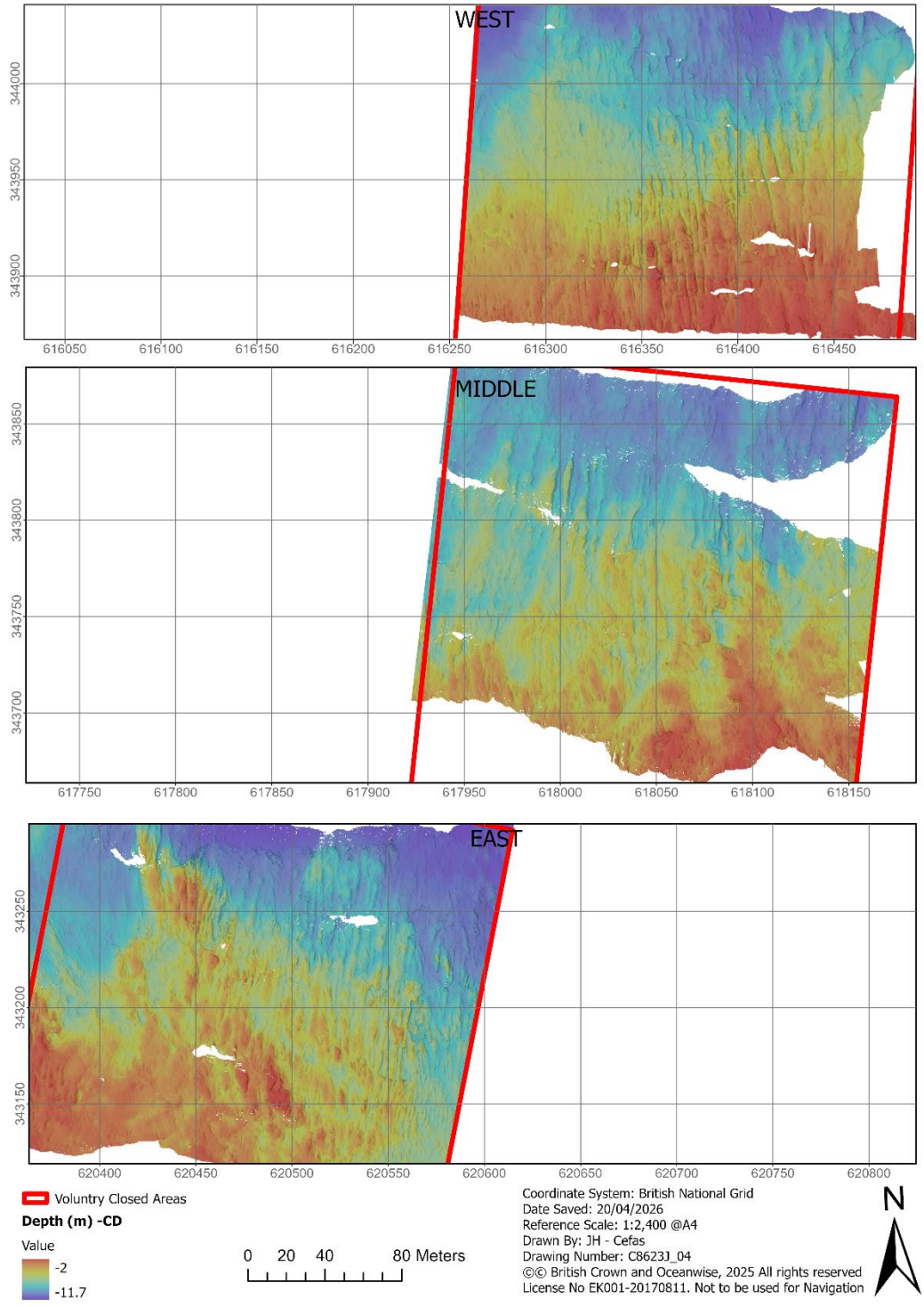

Figure 4. Map showing the masked "Spring 2024" bathymetric datasets from the three experimental areas.

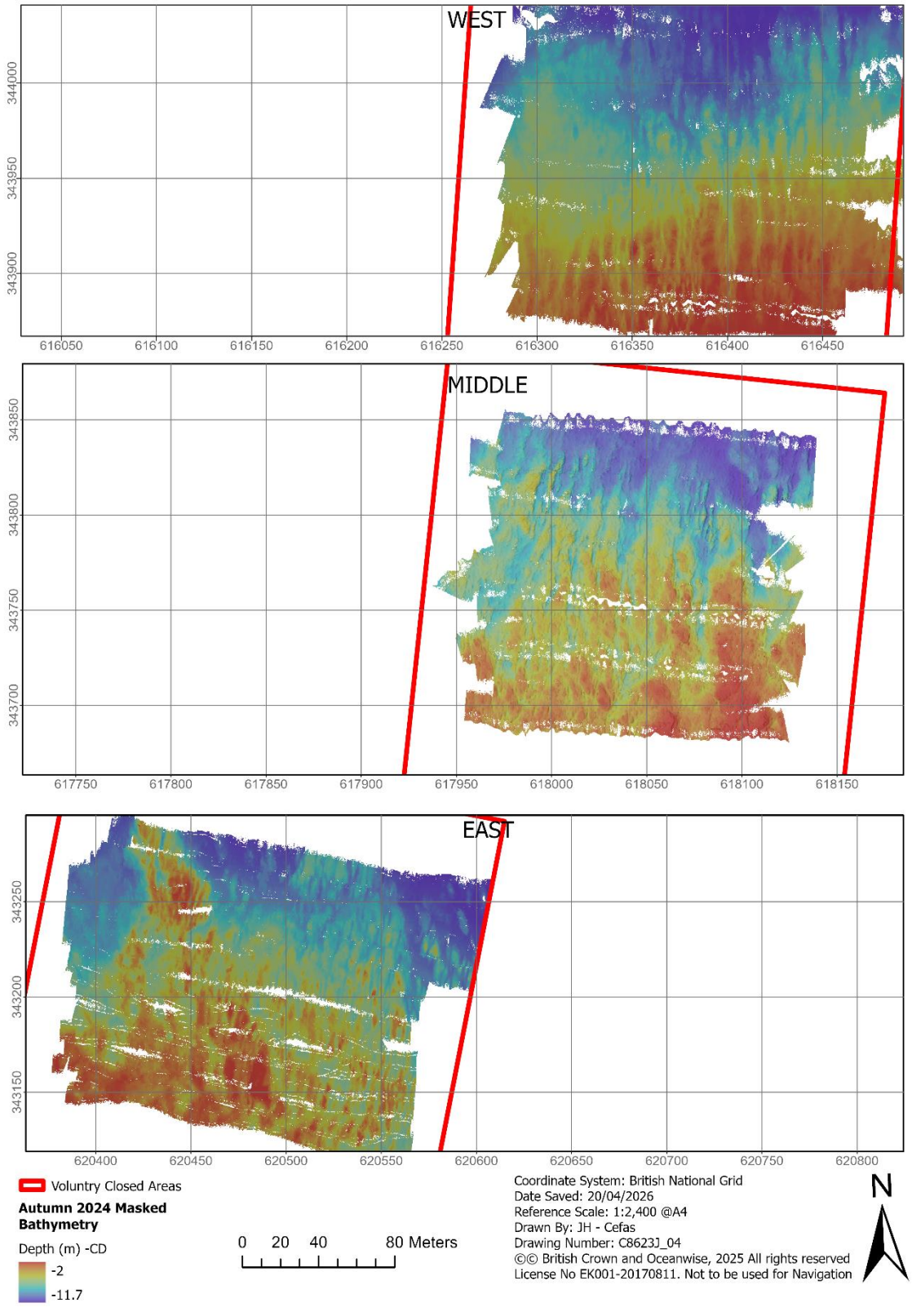

Figure 5. Map showing the masked "Autumn 2024" bathymetric datasets from the three experimental areas.

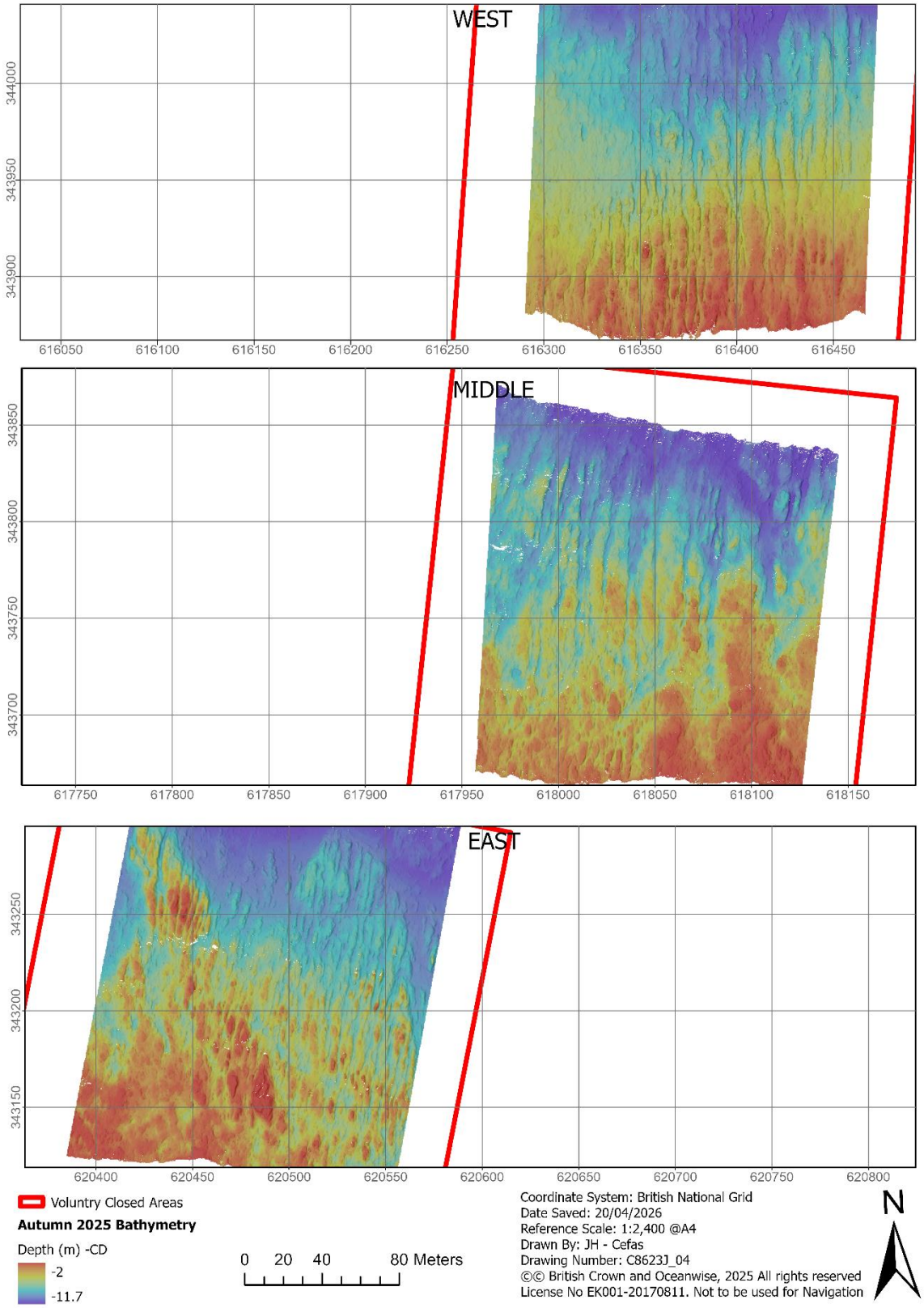

Figure 6. Map showing the masked "Autumn 2025" bathymetric datasets from the three experimental areas.

During the masking and TIN generation process, there was noted a degree of inconsistency within all MBES datasets as regards to horizontal control – with obvious horizontal offsets between clear topographic features (Figure 7).

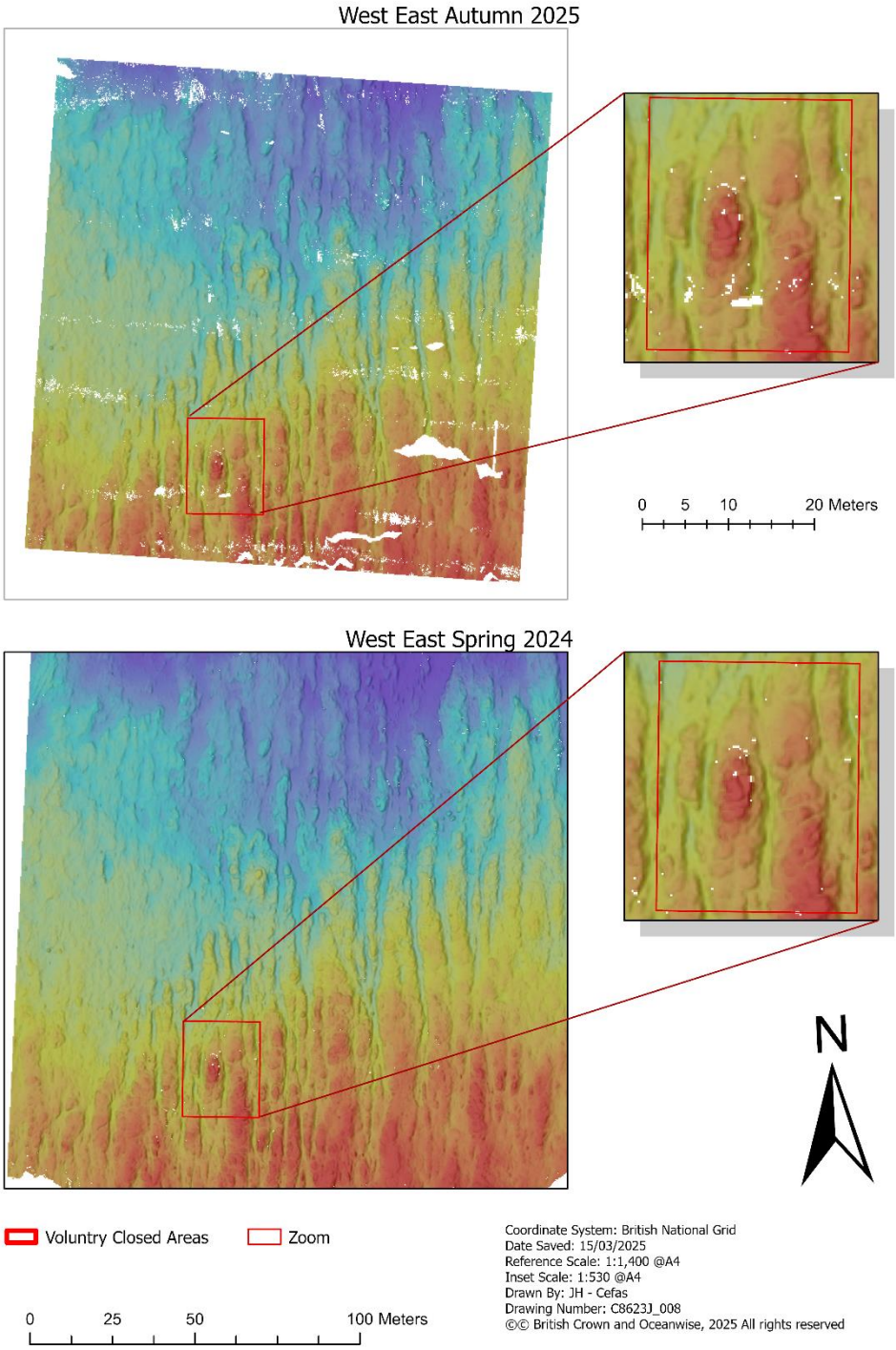

Figure 7. **Map showing the offset between the "Spring 2024" and the "Autumn 2025" bathymetric datasets from the West_East experimental (impact) area.**

Further investigation into this offset was undertaken using the TIN 3D elevation models and gridded bathymetry files in ArcScene (a 3D viewer within ArcMap Pro). The results of this, shown in Figure 8, present in a clear visual the scale of the horizontal offset between the Spring 2024 and Autumn 20254 datasets.

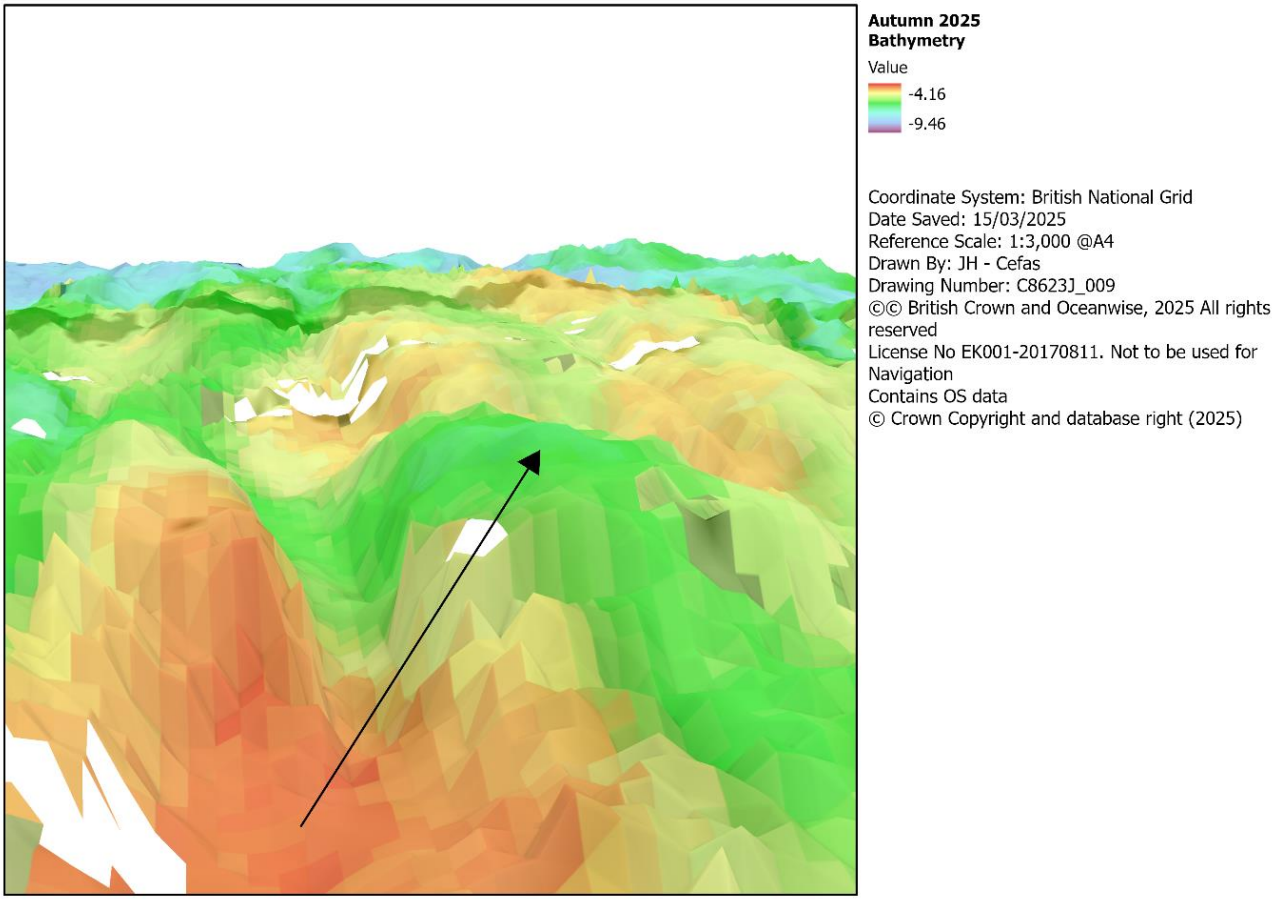

Figure 8. Arc Scene "Spring 2024" and the "Autumn 2025" bathymetric datasets from the West_West experimental (impact) area. This figure shows the colour scale of the 2025 data as laid over the 3-Dimensional elevation from the Spring 2024 dataset – highlighting

Figure 8 shows the 2025 colour grid (bathymetric colour scale, red is shoaler than green) overlying the 3D elevation surface from 2024. The horizontal offset, here appearing to be ~4.5m in scale has resulted in a clear feature mis-match – where the high point (spur) in 2025 corresponds with the low point (groove) in 2024.

This highlights a substantive horizonal positioning offset between the T0 and T1 datasets – specifically a 2 to 5m discrepancy. As the ROV ground truthing data from both years confirms that the substrate (out-cropping chalk reef) has

not changed due to coastal processes such as mobile sediment inundation, this discrepancy is considered to be the product of differences in horizontal control between surveys, related to acquisition horizontal datum. The scale of the offsets is indicative of Real-Time Kinematic (RTK) Global Navigation Satellite System (GNSS) solution loss, with no Post Processed Kinematic (PPK) solution being calculated post-hoc.

3.3. Surface Difference

The identified horizontal offset between bathymetric grids produced for T0 (both datasets) and T1 resulted in much reduced reliability of the surface difference based volumetric comparison, as presented in Figure 9. The outputs clearly show the east-west offset in elevated surface difference values of ~-1.5 and 1.5m maxima being associated with the known spur and groove formations of the rugged chalk.

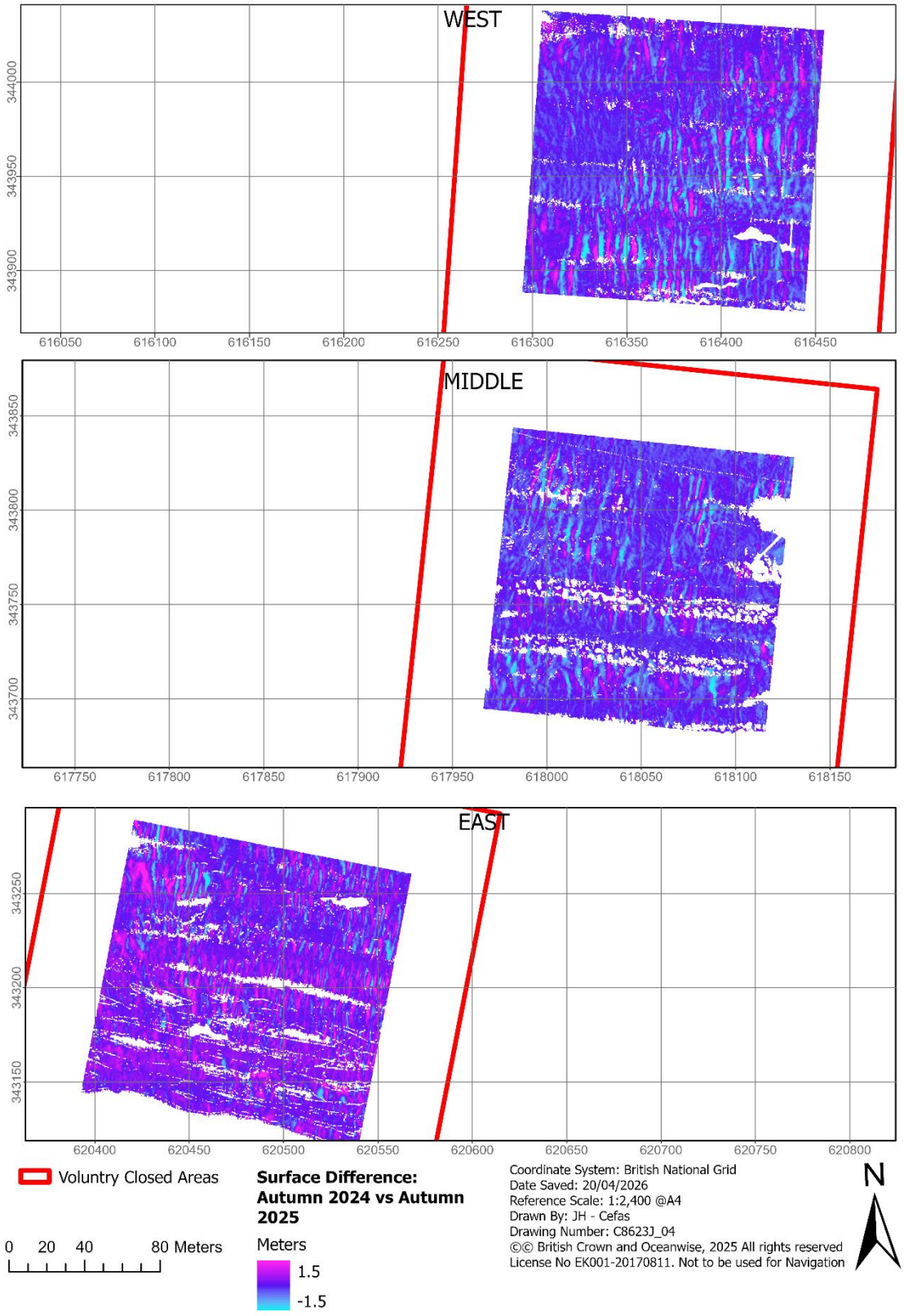

Figure 9 Map presenting the results of the "Surface Difference" analysis between the "Spring 2024" and the "Autumn 2025" bathymetric datasets from all six areas

3.4. Bathymetric Profile Comparison

As the originally proposed Surface Difference methodology was hampered by the uncertainty in horizontal accuracy between T0 and T1 raw MBES datasets, a secondary approach to determination of was trialled. This approach looked at deriving high resolution bathymetric profiles from the track-lines of the ROV ground truthing surveys.

Specific elevations from readily identified reef features (peaks) have been cross referenced and their elevation differences compared.

The results from the profile matching bathymetric grid comparison are presented graphically (Figure 10 in large scale and all profiles in Figure 11) and can be seen provide a detailed assessment of localised morphological change between the 2024 and 2025 bathymetric datasets.

By aligning bathymetric grid profiles with cross correlation (green dotted lines represent the re-aligned 2025 data), matching homologous features through the Hungarian assignment algorithm, and quantifying elevation differences at these matched points, the analysis isolates true geomorphic change from artefacts of survey misalignment or inconsistent sampling. The red lines represent the matched features after cross-correlation process re-aligned the profiles.

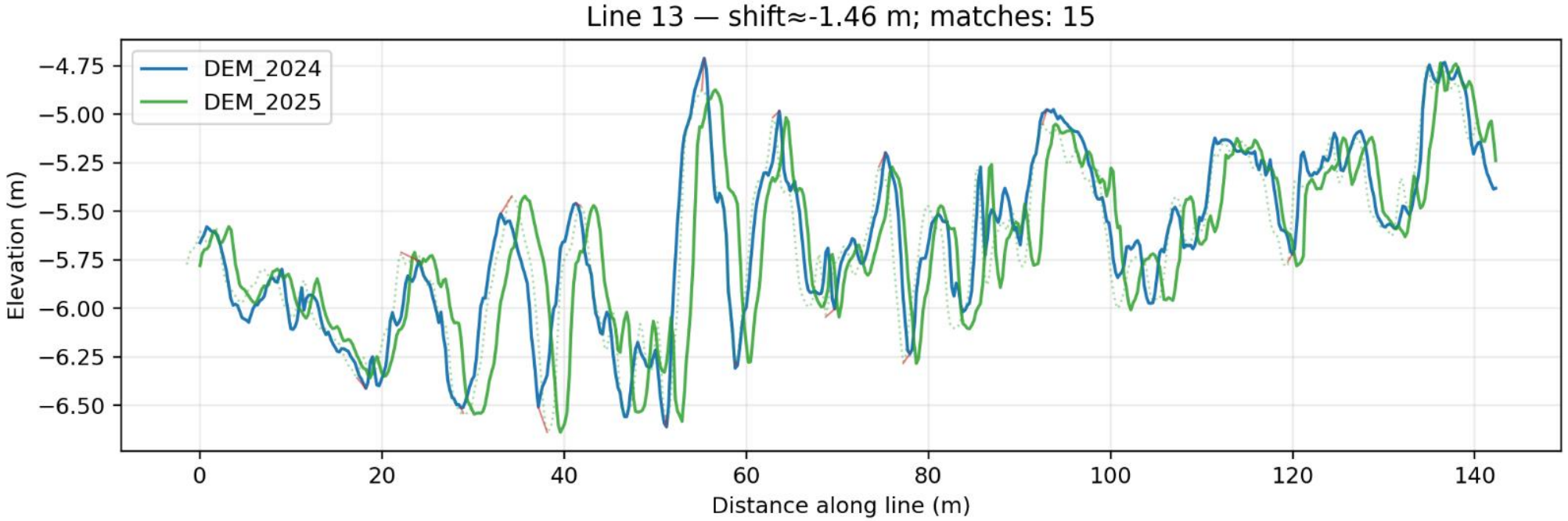

Figure 10 Profile comparisons: Using ROV profiles where impact was observed, the above profiles show the elevations from the same lines between Spring 2024 and Autumn 2025 datasets. Green dotted line represent the re-aligned 2025 data

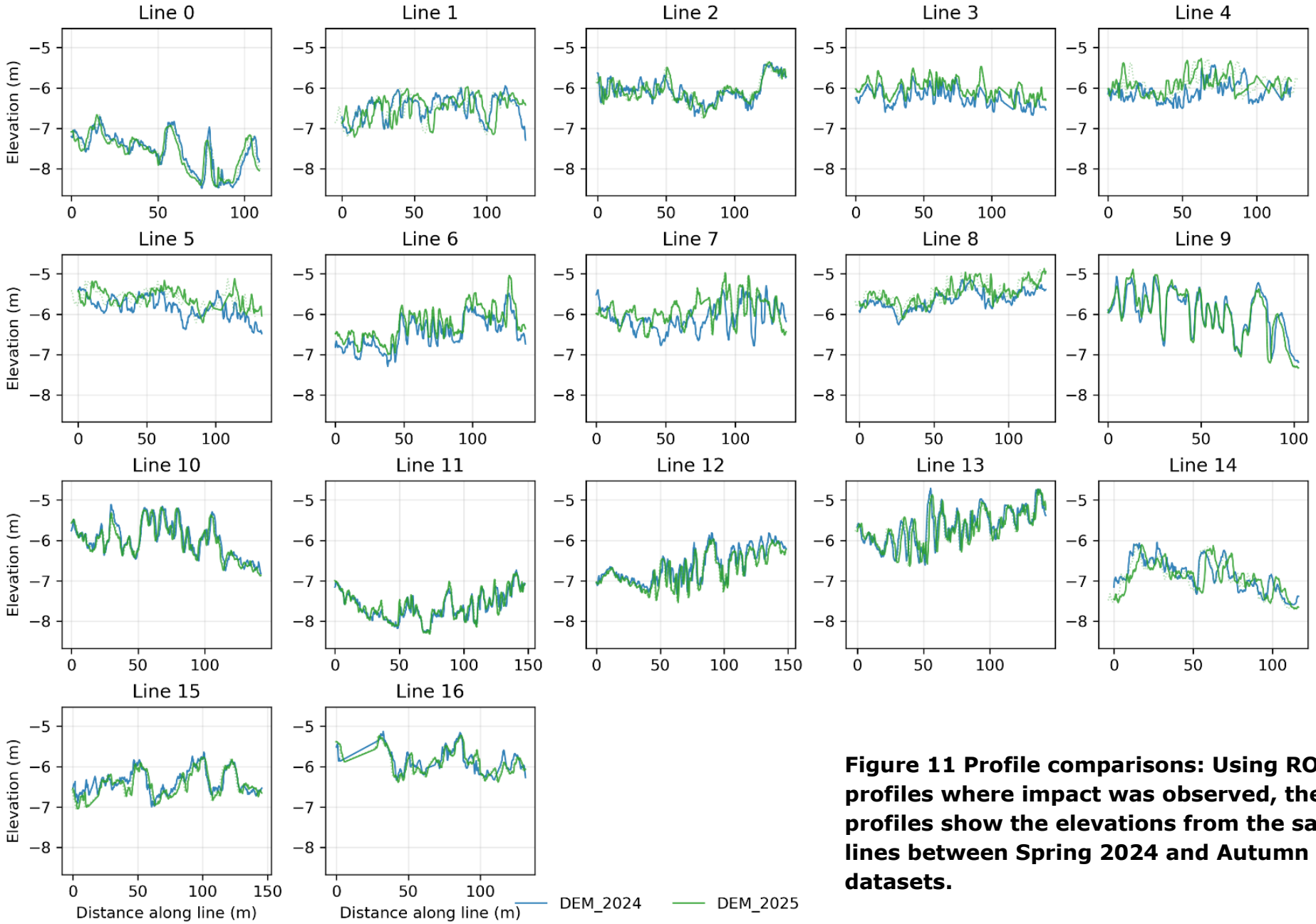

Figure 11 Profile comparisons: Using ROV profiles where impact was observed, the above profiles show the elevations from the same lines between Spring 2024 and Autumn 2025 datasets.

3.4.1. Profile Alignment and Feature Consistency

Across all transects, profiles from the two survey years aligned well after cross-correlation-based horizontal translation. This suggests that any navigational drift or survey-geometry differences were correctable (0.5 to 5m).

The generally low residual horizontal offsets after alignment indicate that matched features between bathymetric grids were physiographically consistent. Where larger residual offsets occurred, it is possible that these may coincide with lower confidence scores or with morphological zones known to be unstable (e.g. near-channel boundaries or mobile sand accumulations).

Given the objective to understand physiographic change of reef (spur and groove) features (which could be morphological features prone to instability) these cases should be interpreted cautiously. However, the limited number of low confidence matched pairs indicates that they do not influence overall conclusions.

3.4.2. Matched Features

The Hungarian matching algorithm paired elevation peaks and troughs objectively, avoiding biases that can arise from nearest-neighbour matching when features are unevenly spaced. Most transects produced a consistent number of matched features between the two years, indicating good morphological continuity. Where the number of matches was reduced, this generally corresponded to areas where one or both bathymetric grids showed very low vertical variability or where complex morphology reduced the prominence of identifiable extrema.

The agreement in feature curvature (shape similarity) and small vertical differences across most matched points, combined with high alignment confidence, supports the reliability of the feature-matching workflow.

3.5. Elevation Change

Vertical change (Δz) was computed at each matched feature as the difference in elevation between the 2025 and 2024 bathymetric grids. These point-wise measurements form the basis for both transect-level and whole-study statistical inference.

3.5.1. Transect-Level Patterns

Some transects displayed small but consistent elevation differences, typically on the order of a few centimetres to decimetres. These localised changes may reflect sediment mobility, small-scale channel adjustment, or seasonal morphological variability. In contrast, several other transects showed negligible Δz across all features, implying stability during the monitoring interval.

The spatial distribution of Δz within individual profiles also provides insight into sediment transport pathways or morphological processes. For example, minor deepening may be evident in troughs while adjacent crest features remain stable, suggesting re-working of material without substantive profile translation.

3.5.2. Mixed-Effects Model Results

The linear mixed-effects model (random intercept) estimates the overall mean elevation change across all transects, the results of which (Table 3) present a mean intercept $\Delta z\,(2025–2024) = 0.047$ m, Std. Err 0.028 [with a Confidence Interval of −0.008 to 0.102m], $p = 0.097$. This result states that, on average, the 2025 data are 4.7cm higher than the 2024 dataset.

Table 3 Summary of the Mixed Effect Linear Model (Random intercept, Restricted Max Likelihood) results to determine significance of change over time in profile matched pair elevation

Model: Mixed LM		**Dependent Variable: Δz**	
Total matched features across all lines: 187			
No. Observations: 188			
No. Total: 17	Scale:	0.0177	
Min. group size: 5	Log-Likelihood:	92.1783	
Max. group size: 20	Converged:	Yes	Mean group size: 11.1
Mean Intercept = 0.048	Std Error = 0.028 CI = 0.092 -0.008 0.103		
Group Var 0.012			
Estimated overall Δz (2025 - 2024): 0.0477 m			
P-value = 0.09223 (>0.05)			

Overall elevation change – the intercept indicated that **no statistically significant change in elevation was observed at p <0.05,** although this value is very close to the P value of 0.05 and the point estimate indicates a small positive elevation difference on average. With a lower confidence P value, this result could be considered significant.

3.6. Predictive Mapping

The predictive classifier model was trained on the four geomorphological classes outlined in Section 2.5:

- Gravel/ Rubble Flat (Class "0")
- Groove (Class "1")
- Mound (Class "2")
- Spur (Class "3")

The results of the testing indicated that the most accurate model run was an 'Linear Discrimination Analysis' (LDA). Feature (i.e. data layer) importance for the final predictive model was presented (*post-hoc*) using the 'Feature

Importance Plot' algorithm, available in PyCaret. This algorithm uses a combination of several supervised feature selection techniques to select the subset of features that are most important for modelling. Figure 12 presents the results of this selection, showing that the standard deviation of the Rugosity Index "RI" (sd_RI) was found to be the most informative (FIGURE XX), followed by the mean object Rugosity Index "RI" (Mean_ri). Explanations of these data layers can be found in Section 2.5.

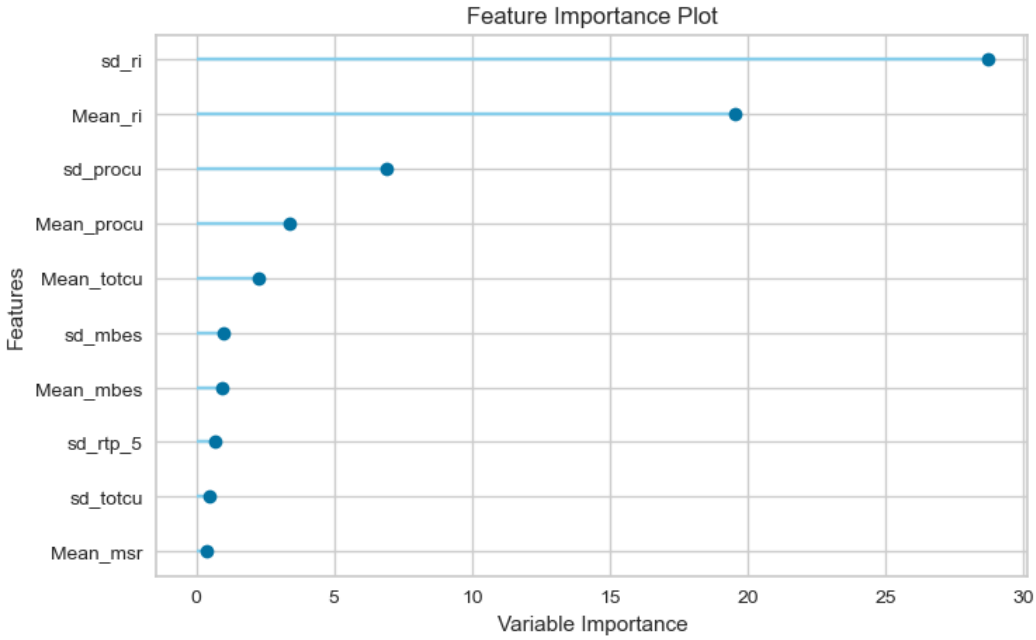

Figure 12 Feature Importance for the developed predictive classifier model

During cross fold validation, a class-confusion matrix was computed using the held back validation subset. This confusion matrix is presented in Figure 13 , and shows that classes 0 (Gravel / Rubble Flat) and 3 (Spur) were best conserved (i.e. had the leas between class confusion). With Class 1 ("Groove") being occasionally confused with Class o (Gravel/Rubble Flat).

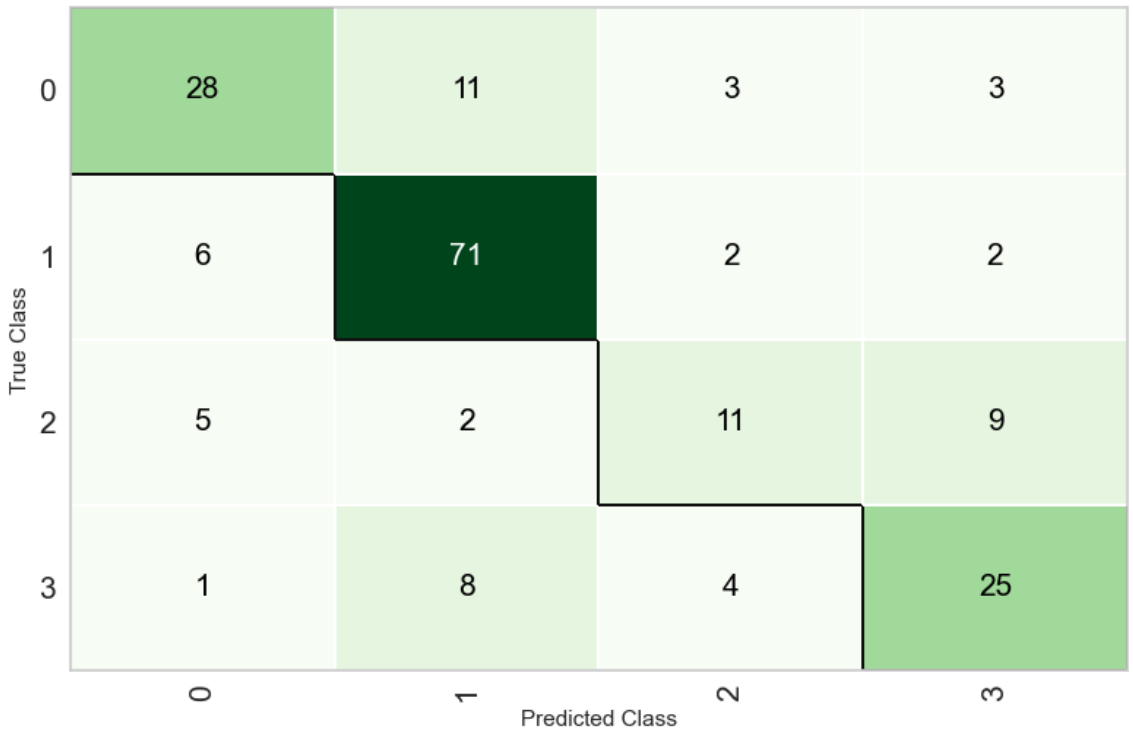

Figure 13 Confusion Matrix for the final LDA predictive classifier model with four classes.

3.6.1. Cross-validation and accuracy

Results from the 10-fold cross-validation of the final Linear Discrimination Analysis' (LDA), are presented in Table 4 which shows an overall high level of both producers (Recall) and user's (Precision) accuracies (71 % and 74%) for the model.

Table 4 Cross Validation Accuracy of the LDA classifier model

Model	Accuracy	AUC	Recall	Prec.	F1	Kappa	MCC
Linear Discrimination Analysis –'LDA'	0.7062	0.7903	0.7062	0.7447	0.7191	0.3641	0.371

3.6.2. Geomorphological maps

The outputs of the trained predictive classifier are presented here in Figure 14 and Figure 15.

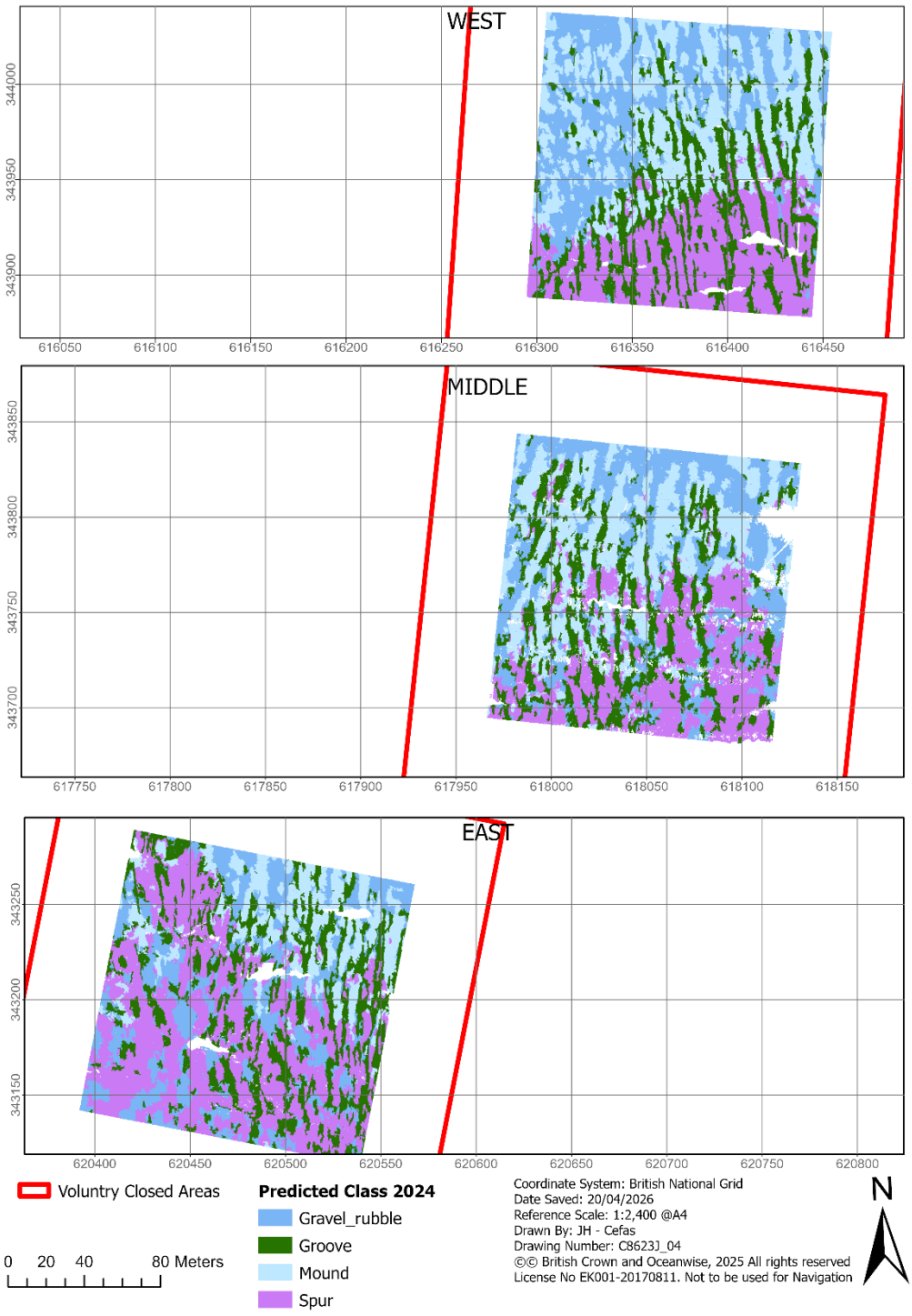

Figure 14. Geomorphological classifications for each of the 6 experimental areas as observed in the Spring 2024 dataset.

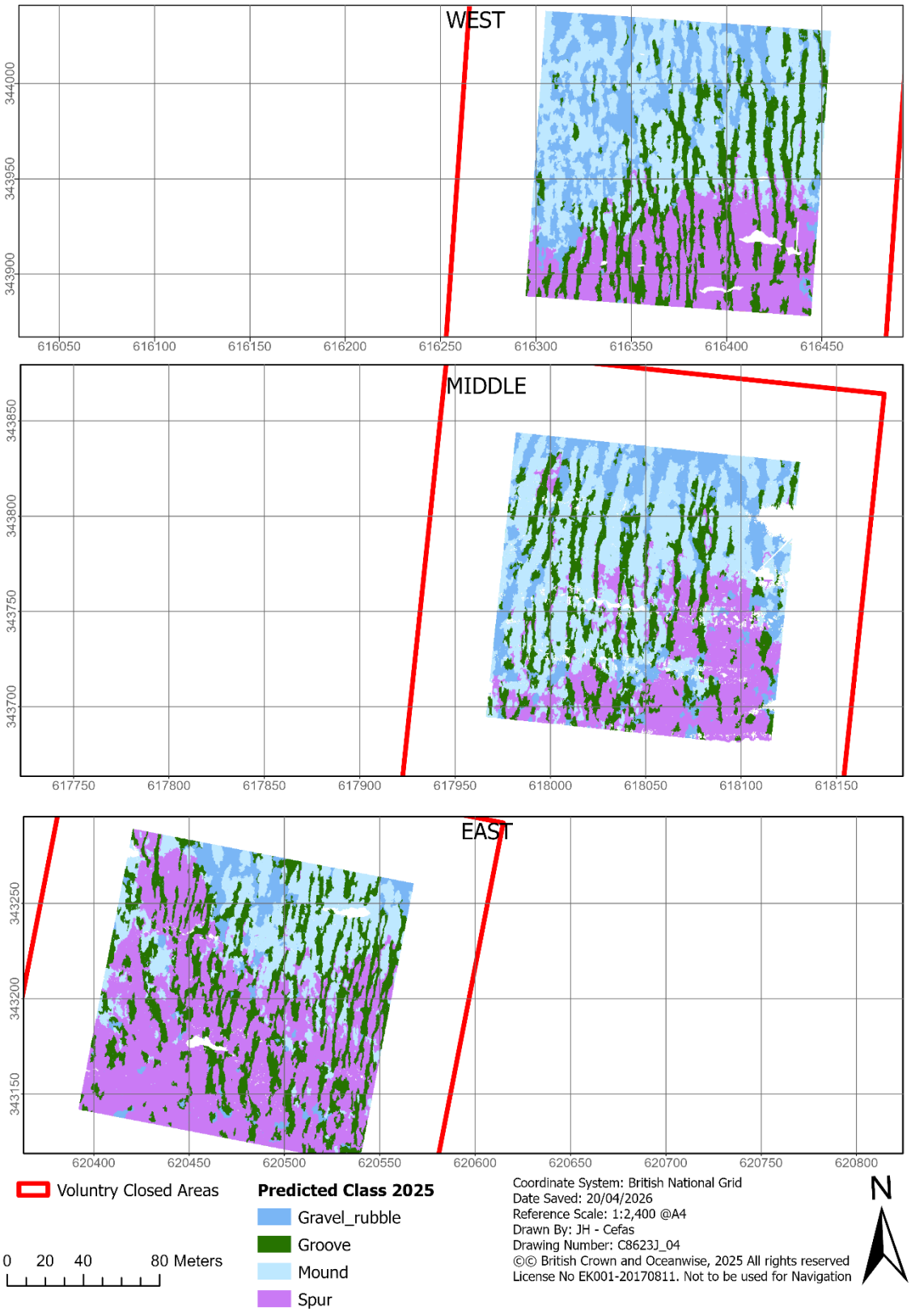

Figure 15. Geomorphological classifications for each of the 6 experimental areas as observed in the Autumn 2025 dataset

4. Conclusion

The work presented in this report has met with the initial objectives of the study in producing multibeam bathymetry derived backscatter layers for T0 and T1 defined timepoints.

Structural complexity analysis has been undertaken using gridded bathymetry, various topographic derivatives and backscatter layer as predictors to train an OBIA deployed geomorphological classifier algorithm for the site. This classifier has been deployed across the T0 and T1 datasets and has classified the experimental areas as one of five classes:

- Groove
- Spur
- Mound
- Gravel/ Rubble Flat

This very high-resolution model (0.25m) will provide stakeholders and managers with a clearer outline of where "Rugged Chalk" is located within the experimental areas. Specifically, we propose collating the "Spur" and "Groove" classes into a function management class of "Rugged Chalk".

Bathymetric surface difference (volumetric method) maps were produced, however due to issues with horizontal control of the raw bathymetry data, these maps are of limited confidence.

As such, a secondary method of bathymetric difference comparison between T0 and T1 time points was undertaken – that of statistical profile comparison. This method matched the elevation points from transects across both T0 and T1 datasets, then compare the elevations of these matched pairs statistically. We recommend that these results are considered indicative until such time as the horizontal control of the bathymetric grids can be amended. However, this indicative method indicated that, at the 0.25m resolution, no significant changes in elevation can be inferred between T0 and T1.

We recommend that further investigation be paid into the horizontal control of the raw hydrographic datasets, with a view to assessing if alignment is possible given the identified acquisition or processing artefacts which have resulted in the observed offset. The resolution of the 0.25m gridded datasets can be considered sufficient to observe large scale (>25cm^2) abrasive impacts, however we cannot state if the site wide surface difference approach would be successful, owing to the observed horizontal offsets.

Given the quality and resolution (0.04m) of the backscatter datasets, further work is proposed focussing on secondary predictive mapping of each backscatter dataset (T0, T1 and intervening surveys). We suggest using the predictive geomorphological maps produced in this report to subset the backscatter data into "rugged chalk", then undertake OBIA with unsupervised classification to identify candidate impact features . Noting that the rugged chalk is predominantly associated with a more reduced backscatter intensity, we anticipate this approach will be able to isolate small patched of increased backscatter intensity within areas of topographically rugged chalk. Cross referencing these small patches of high reflectance with ground truth data may enable the detection and mapping of impact forms.

5. References

Blaschke, T., 2010. Object based image analysis for remote sensing. ISPRS J. Photogramm. Remote Sens. 65, 2–16. https://doi.org/10.1016/j.isprsjprs.2009.06.004

Bracewell, R. (1999). *The Fourier Transform and Its Applications.*

Dove, D., Nanson, R., Bjarnadóttir, L.R., Guinan, J., Gafeira, J., Post, A., Dolan, M.F.J., Stewart, H., Arosio, R., Scott, G., 2020. A two-part seabed geomorphology classification scheme: (v.2).

Florinsky, I.V., 2017. An illustrated introduction to general geomorphometry. Prog. Phys. Geogr. Earth Environ. 41, 723–752. https://doi.org/10.1177/0309133317733667

Lindsay, JB., 2014. The Whitebox Geospatial Analysis Tools project and open-access GIS., in: Proceedings of the GIS Research UK 22nd Annual Conference. The University of Glasgow. https://doi.org/10.13140/RG.2.1.1010.8962.

Kuhn, H. (1955). "The Hungarian method for the assignment problem." *Naval Research Logistics Quarterly.*

Lewis, J. (1995). "Fast normalized cross-correlation." *Vision Interface.*

Lucieer, V., Lamarche, G., 2011. Unsupervised fuzzy classification and object-based image analysis of multibeam data to map deep water substrates, Cook Strait, New Zealand. Cont. Shelf Res. 31, 1236–1247. https://doi.org/10.1016/j.csr.2011.04.016

Munkres, J. (1957). "Algorithms for the assignment and transportation problems." *Journal of the Society for Industrial and Applied Mathematics.*

Newman, D.R., Lindsay, J.B., Cockburn, J.M.H., 2018. Evaluating metrics of local topographic position for multiscale geomorphometric analysis. Geomorphology 312, 40–50. https://doi.org/10.1016/j.geomorph.2018.04.003

Olofsson, P., Foody, G.M., Herold, M., Stehman, S. V., Woodcock, C.E., Wulder, M. a., 2014. Good practices for estimating area and assessing accuracy of land change. Remote Sens Env. 148, 42–57. https://doi.org/https:/doi.org/10.1016/j.rse.2014.02.015itle

Phinn, S.R., Roelfsema, C.M., Mumby, P.J., 2012. Multi-scale, object-based image analysis for mapping geomorphic and ecological zones on coral

reefs. Int. J. Remote Sens. 33, 3768–3797. https://doi.org/10.1080/01431161.2011.633122

Pinheiro, J. & Bates, D. (2000). *Mixed-Effects Models in S and S-PLUS.*

Roelfsema, C., Phinn, S., Jupiter, S., Comley, J., Albert, S., 2013. International Journal of Remote Mapping coral reefs at reef to reef- system scales , 10s – 1000s km , using. https://doi.org/10.1080/01431161.2013.800660

SciPy Library Documentation

Savitzky, A., & Golay, M. (1964). "Smoothing and Differentiation of Data by Simplified Least Squares Procedures."

Stephens, D., Diesing, M., 2015. Towards quantitative spatial models of seabed sediment composition. PLoS ONE 10, 1–23. https://doi.org/10.1371/journal.pone.0142502

Zuur et al. (2009). *Mixed Effects Models and Extensions in Ecology with R.*

Tackling global challenges through innovative science solutions

Cefas, the Centre for Environment, Fisheries and Aquaculture Science, is an Executive Agency of Defra (the UK Government's Department for Environment, Food and Rural Affairs).

Through innovative solutions and world-leading applied science we work to ensure a sustainable future for our rivers, seas and the ocean, supporting healthy and productive marine and freshwater ecosystems.

Centre for Environment, Fisheries & Aquaculture Science

Cefas

Pakefield Road, Lowestoft, Suffolk, NR33 0HT, UK

The Nothe, Barrack Road, Weymouth, DT4 8UB, UK

www.cefas.co.uk | +44 (0) 1502 562244

OGL

LRQA CERTIFIED ISO 9001:2015 LRQA CERTIFIED ISO 45001 disability confident LEADER